[1]Mainak Mallik

[2]Saurabh Dubey

[2]Deepak Gupta

Machine Learning Approach to Forecast the Tensile Strength of Bamboo

Abstract: - Bamboo holds significant global economic importance as a non-timber forest product. Its fibers can be utilized in concrete reinforcement, a concept known as bamboo fiber reinforced concrete. Nevertheless, further investigation is required for Bamboo Fiber Reinforced Concrete, with a specific focus on bamboo tensile strength. This study aimed to foretell the BTS through several machine learning techniques, including artificial neural network, extreme learning machine, and support vector regression. A total of 30 samples from the previous literature article were considered for predicting Bamboo Tensile Strength. The dataset was split into two parts, with 80% allocated for training data and 20% for testing data. The outcome from the data testing shows that the extreme learning machine predict very sensitive to random errors in the observed target. The results show that a positive correlation was found between key input parameters, such as the shorter dimension of bamboo, the longer dimension of bamboo, cross- sectional area, modulus of elasticity, and area, in relation to the output bamboo tensile strength.

Keywords: Artificial Neural Network (ANN), Bamboo Tensile Strength (BTS), Extreme Learning Machine (ELM), Machine Learning (ML), Support Vector Regression (SVR)

I. INTRODUCTION

Bamboo, a sustainable and environmentally friendly resource, has a long-standing tradition of being utilized in housing construction across various regions including Asia, the Pacific Islands, the United States of America, and Africa. Notably, bamboo exhibits rapid growth, with young bamboo shoots capable of reaching impressive daily growth rates of around 21-30 cm [1]. Bamboo faces strong competition from reinforced concrete, masonry, and steel, which are commonly seen as superior materials. However, considering that bamboo grows in the regions where urbanization will primarily occur in the 21st century, reshaping perceptions and promoting its use could have a profound impact on carbon emissions, safety in construction, and the overall quality of life in these countries. Bamboo has the potential to make a significant difference in shaping a sustainable and high-quality built environment for the future [2]. Promoting the use of recombinant bamboo furniture offers an efficient solution to address the shortage of wood resources. Recombinant bamboo surpasses ordinary timber in terms of mechanical strength and exhibits beautiful grain color. Additionally, its processability is similar to hardwood, making it an optimal material for furniture manufacturing in China [3]. The size effect coefficients were calculated using the slope mode and the variable mode. The results favored the Linear Regression (LR) parameter analysis as the more suitable approach for assessing the size effect. The coefficients obtained were 0.043 for compressive strength ($R^2 = 23.26$), 0.064 for elastic modulus ($R^2 = 15.63$), 0.0529 for ductility coefficient ($R^2 = 18.90$), and 0.133 for compression coefficient ($R^2 = 7.52$). Notably, the Compressive Strength (CS) of laminated bamboo lumber is less affected by the size effect compared to wood [4]. Hitam, Andong, and Tali bamboo culms can be structurally graded for compressive load using either strength or capacity grading methods, as both show a strong correlation with the indication forecaster. However, capacity grading is preferred due to its strongest correlation with linear mass (q), which directly relates to compressive load-carrying capacity [5]. The mechanical properties of bamboo scribers exhibit notable variations based on both the density of the material and the orientation of its fibers. The dynamic MoE was assessed for the first time in both parallel and perpendicular fiber directions. Additionally, the long-term water absorption results showed significant variability depending on the specimen's density. These findings are of great importance for advancing the production and application of bamboo scribers with uniform density [6]. The study findings suggest that considering the duration of

[1] Author: mainak.mallik@gmail.com

[2] *Corresponding author: saurabhmmmec21@gmail.com

[3] Author: deepakjnu85@gmail.com

[1,2] National Institute of Technology, Arunachal Pradesh-791113, India

[3] Motilal Nehru National Institute of Technology, Allahabad-211004, India

exposure to humidity can be beneficial in constructing bicycle frames, as it allows for leveraging the variations in strength between dry and wet conditions. This knowledge can be applied to optimize the performance and durability of bicycle frames [7]. The compressive stress-strain curves of bamboo scriber remain linear below the proportional limit. Beyond this limit, they become nonlinear, especially at elevated temperatures. Along the grain direction, the compressive modulus and strength reduces with increasing temperature until 200°C, where a sudden increase is observed [8].

Researchers have achieved significant breakthroughs in bamboo-mimetic materials and structures. Bamboo serves as a promising biomimetic model, enhancing energy absorption, physical properties, and structural durability. It also enables mass reduction in structures and composite materials. Bamboo-mimetic design improves toughness, physical durability, and surface area for specialized materials [9]. Biochar mortars outperform the control mortar in terms of compressive strength. The best strengthening effect is achieved with a 1% replacement of bamboo biochar in cement. Replacing 1-4% of bamboo biochar brings significant and stable improvements to the CS of biochar mortar [10]. CS of bamboo specimens gradually decreases from -60°C to 200°C. High temperatures thin the cell wall, leading to the loss of the layered structure and reduced bearing capacity. The study's empirical formulas can estimate compressive strength changes in high or low temperatures [11]. A physical and mechanical analysis of Gigantochloa scortechinii bamboo (45-60 mm diameter) revealed higher moisture content in the bottom section, increasing density towards the top section, and a positive correlation between culm wall thickness and strength. Nodes exhibited greater strength than internodes along the bamboo culm [12]. The CS parallel to the grain is 2.1 times higher than the CS perpendicular to the grain. Similarly, the elastic modulus for compression parallel to the grain is 3.64 times greater than the elastic modulus for compression perpendicular to the grain. The compression ratios are equal in both directions. In terms of Poisson ratios, one typical side surface has a value of 3.93 times larger than the other for PBSL specimens under compression perpendicular to the grain. However, the larger Poisson ratio is equivalent to that observed for PBSL specimens under compression parallel to the grain [13]. The application of preservative treatment had a notable effect on the physical and mechanical attributes of Gigantochloa scortechinii strips. Compared to boron treatment, using copper chrome boron (CCB) preservatives resulted in a higher Modulus of Rupture (MoR) and CS for the treated bamboo. This indicates a positive influence on the suitability of bamboo, especially in structural applications [14]. Scanning electron microscopy (SEM)-energy dispersive X-ray (EDX) analysis revealed that an increase in bamboo fiber content without a corresponding increase in natural rubber latex content resulted in the formation of void spaces within the concrete. This led to a decrease in strength, indicating the importance of maintaining the appropriate balance between bamboo fiber and natural rubber latex content for optimal concrete performance [15]. The addition of bamboo fiber to concrete increases its flexural strength by approximately 10% compared to traditional concrete. Initially, the concrete strength improves with a minor quantity of fiber (0.5%). However, further addition of fiber leads to a reduction in the strength. As flexural capacity is directly related to tensile strength, the experimental results indicate that an increase in flexural strength enhances tensile concrete strength [16].

In this study, an empirical formula combining exponential and sine functions is proposed to foretell the off-axis CS of laminated bamboo. The formula's accuracy is compared with other commonly used failure criteria. The results indicate that the proposed empirical formula and the Hankinson formula with n = 1.5 provide more precise predictions for the off-axis CS of laminated bamboo [17]. The Fourier Transform Infrared Spectroscopy (FTIR) test results revealed that a temperature of 175°C acted as a significant turning point, causing thermal decomposition of cellulose in bamboo and phenolic compounds in the resin. This information can be valuable in estimating the fire behavior of bamboo structures through numerical analysis and predicting the material's residual load capacity [18]. The physical, chemical, and mechanical attributes of bamboo change significantly during saturated steam heat treatment, depending on the treatment duration and initial Moisture Content (MC). Bamboo initially becomes more crystalline during treatment, peaking in crystallinity at an initial moisture content of 40%. This process involves the breakdown of hemicellulose and non-crystalline cellulose, along with the creation of cellulose ether bonds between hydroxyl groups, resulting in increased hydroxyl content that gradually declines over time [19]. The key performance indicator and growth parameters of bamboo, including wall thickness and outer circumference, were fitted using linear, exponential, and power functions. The results indicate that the longitudinal physical characteristics, bending, and transverse CS of inter-node samples reduces as wall thickness and outer circumference increase. On the other hand, the transverse CS of nodal samples and the transverse tensile strength of both nodal and inter-node samples increase with an increase in wall thickness and outer circumference [20]. The single bamboo tube Reinforced (R/F) foam structure illustrates the highest specific energy absorption and CS. Increasing the foam density further enhances these values. Additionally,

a larger diameter of the bamboo tube improves both specific energy absorption and CS [21]. Bamboo scriber exhibits superior strength and stiffness compared to other wood- and bamboo-based products, making it a viable substitute for wood in structural applications. Through heat treatment and the addition of phenolic resin, bamboo scriber also gains resistance to mold and decay, making it suitable for exterior use. Applications such as exterior flooring, trestles, and pavilions can take advantage of bamboo scriber's high strength and abrasion resistance [22]. The initial CS parallel to the grain for unprocessed specimens is 89.07 MPa. With increasing oil heat treatment temperature, the CS initially increases and then decreases. The samples reach their maximum CS parallel to the grain (109.52 MPa) after being treated with oil at 160°C for 2 hours. This maximum strength is 18.63% higher than that of untreated samples, but it begins to decline thereafter. When the temperature reaches 200°C, the CS parallel to the grain of the oil heat-treated specimens is lower than that of the unprocessed samples [23]. The extensive performance of 33 bamboo blocks with different vascular bundle volume fractions (Vvb) across the culm wall thickness was examined. All samples displayed similar stress-strain curves, consisting of an elastic stage, elastic-plastic stage, and purely plastic stage before reaching crushing. SEM observation revealed that fiber buckling was the dominant failure mode of the bamboo blocks. The compressive strength and stiffness exhibited a linear increase with Vvb, which can be attributed to the contribution of the strong and brittle vascular bundles [24]. Moso bamboo demonstrates a prominent anisotropic nature in its mechanical attributes, particularly in parallel-to-grain tensile attributes and bending attributes. The parallel-to-grain CS, tensile strength, and bending strength significantly outperform the perpendicular-to-grain mechanical properties. As a renewable and eco-friendly building material, Moso bamboo offers exceptional advantages such as high strength, high stiffness, and an excellent strength-to-weight ratio [25]. ISO has indeed developed standards and codes for bamboo as a construction material. These standards include various tests to find out the physical properties and structural characteristics of bamboo. However, there is still a need for further standardizations and specifications to ensure consistent and widespread use of bamboo in the construction industry. Ongoing efforts in this area aim to enhance the dependability and applicability of bamboo as a reliable and sustainable building material [26].

In the rest of the paper, Section 2 includes the related works, Section 3 labels the description about the dataset. Section 4 discusses the experimental work as a comprehensive comparison between ANN, SVR, and ELM to assess their effectiveness in predicting BTS. In the last section, we conclude our paper with possible future directions.

II. RELATED WORK

A. Artificial Neural Network (ANN): - Artificial Intelligence (AI) heavily relies on ANNs, which were originally created by McCulloch and Pitts [27]. ANN are advanced systems for processing data, stirred by the structure and functioning of the human brain [28]. ANNs consist of fundamental components known as nodes or neurons, and these nodes collaborate to form layers. The connections between neurons, referred to as connection links, carry different weights. Neurons receive inputs and compute a weighted sum, utilizing a unique transfer function, also called an activation function. When this weighted sum surpasses a specified threshold, an output signal is generated. The information flows in a forward direction, hence the term "feed-forward." To diminish the error between output and desired variables, gradient descent and backpropagation algorithms are frequently employed. Figure 1 provides a simplified representation of the suggested network design. The suggested ANN model consists of three layers, and the LMBP model was employed for training. The ability of an ANN to learn is a crucial factor in predicting bond strength. By utilizing a set of input/output data, an ANN can construct a non-linear structure to capture the underlying patterns [29]. The strong point of the FRP-concrete connection has been effectively predicted using ANN in various studies [30].

In the neural network, every neuron in a layer accepts inputs from the layer above it, computes the weighted sum of those inputs, and deploys an activation function to generate outputs that are passed to the next layer.

The set of input parameters represented by $N = (n_1, n_2, n_3 ....n_n)$ are multiplied with weight vector $M_j = (m_{j1}, m_{j2}, m_{j3} ....m_{jn})$ and the following equation will be generated which is given below:

$$T_j = \sum_{i=1}^{n} M_{ji} n_i + b_j \qquad (1)$$

where T_j is the total weight of output.
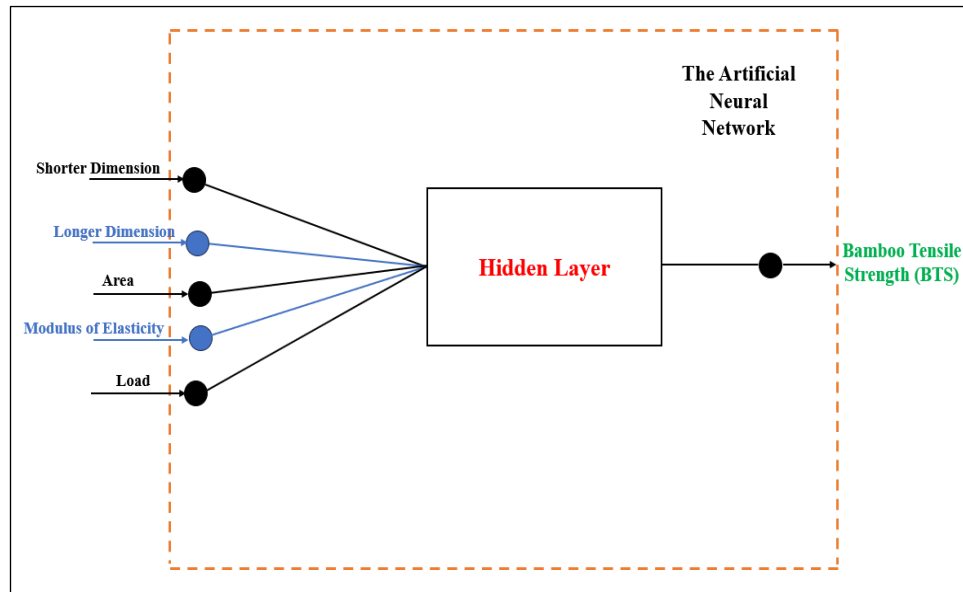
Figure 1: Typical Structure of an ANN

B. Support Vector Regression (SVR): - SVR is an enhancement of the SVM technique for regression, initially introduced by Drucker [31]. The core concept of SVM involves identifying a hyperplane with the maximum distance to the closest data points on either side [32-33]. Similarly, the SVR model aims to generate a hyperplane that diverges by no more than ε for each training point x_i as shown in Figure 2. The hyperplane $A = w.\varphi(y) + b$ can be determined by solving the following quadratic programming problems (QPPs) in such a way:

$$\min_{w,b,\lambda_1,\lambda_2} \frac{1}{2} \| w \|^2 + C(e^t \sigma_1 + e^t \sigma_2)$$

subject to:

$$y_i - (\phi(x_i)w + be) \le \varepsilon e + \sigma_{1i} \quad , \quad \sigma_{1i} \ge 0 \quad ,$$

$$(\phi(x_i)w + be) - y_i \le \varepsilon e + \sigma_{2i} \quad , \quad \sigma_{2i} \ge 0 \quad \text{for } i = 1,...,m$$

(2)

where, slack variables are $\sigma_1 \in (\sigma_{11},...,\sigma_{1m})^t$ and $\sigma_2 \in (\sigma_{21},...,\sigma_{2m})^t$; input parameters a $C > 0, \varepsilon > 0$ [34].

In this context, *w* and *b* indicate the unknown parameters of the hyperplane, while $\varphi(y)$ is a mapping function that transforms *x* into a high-dimensional space. The hyperplane serves as the line employed for predicting the continuous target. In this paper, the radial basis function (RBF) kernel is utilized:

$$K(e_i, f_j) = \exp(-\mu \| e_i - f_j \|^2)$$

In this case, e_i and e_j represent two samples, μ is a kernel parameter and $\| \cdot \|^2$ signifies the squared Euclidean distance between the two feature vectors. The objective is to determine suitable values for *m* and *b* in order to minimize the empirical error with respect to the ε-insensitive loss function. Figure 2 shows the basic structure of SVR.
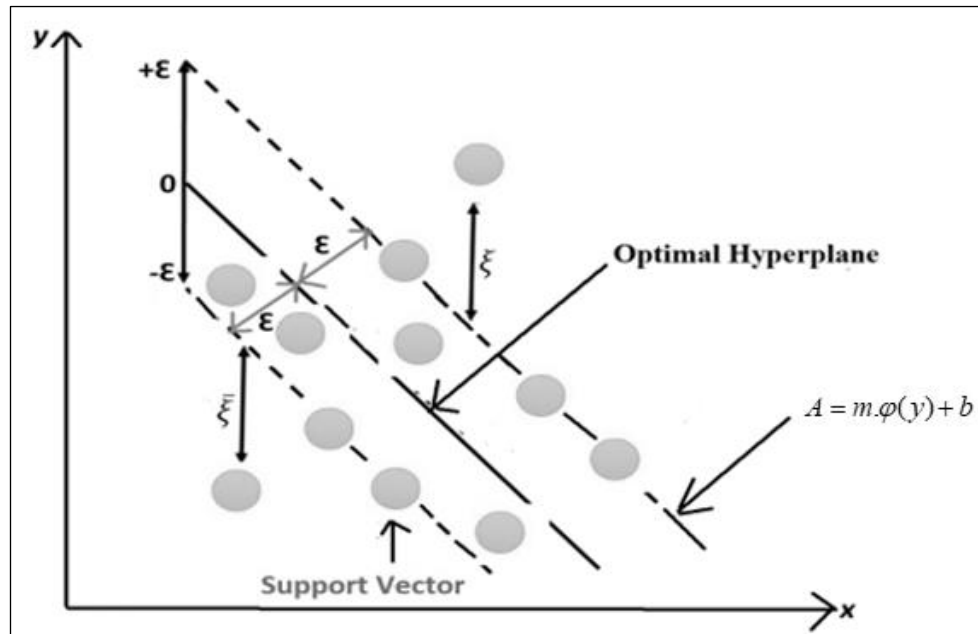
Figure 2: Representation of the structure of the Support Vector Regression (SVR) method

C. Extreme Learning Machine (ELM): - In 2006, Huang et al. introduced the ELM as an AI technique for the construction of single-layer feed-forward neural networks (SLFNs). In ELM, the input weights are randomly allocated, whereas the output weights are methodically determined [35]. The ELM model offers a significant advantage in terms of its design simplicity and efficiency in solving regression or classification problems within a shorter timeframe. This advantage stems from the randomization of weights and biases in its hidden neurons and the utilization of the Moore-Penrose inverse function to obtain a unique least squares solution for the output. The reduced complexity and the analytical solution provided by the ELM contribute to its efficient performance in various tasks [36]. The basic structure of the ELM model is depicted in Figure 3.
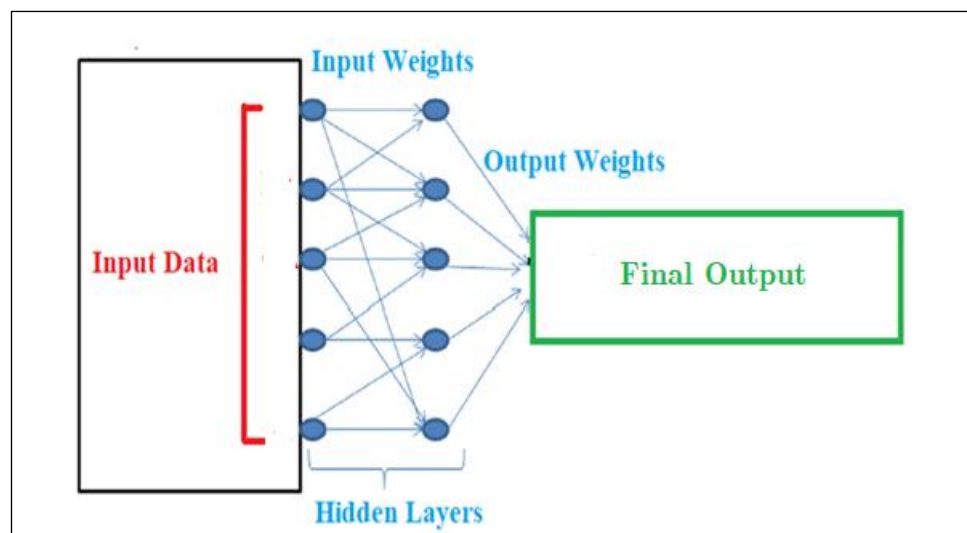
Figure 3: Framework of ELM Technique

For any input data points $x_i = (x_{i1},...,x_{1n})^t \in R^n$ and its output $y_i \in R$ the primal expression can be shown as:

$$y_i = \sum_{k=1}^{L} \eta_k S(\alpha_k, \beta_k, x_i) \quad \text{for } i = 1, 2, 3, 4...m, \tag{3}$$

where $S(\alpha_k, \beta_k, x_i)$ is the non-linear piecewise continuous function which is the outcome of the kth concealed node for the input sample x_i. The randomly assigned input weight vector is denoted as $\alpha_k = (\alpha_{k1},...,\alpha_{kn})^t \in R^n$ and

the bias is $\beta_k \in R$ which connects the input layer to the kth concealed node. The output weight vector is considered as $\eta = (\eta_1,...,\eta_L)^t \in R^L$ which connects concealed layer nodes to the output node where L is the total number of concealed nodes. Further, we can write above (3) in matrix form in this way

$$H \eta = y,$$

(4) where the concealed layer output matrix is introduced as,

$$H = \begin{bmatrix} S(\alpha_1,\beta_1,x_1) & ... & S(\alpha_L,\beta_L,x_1) \\ . & ... & . \\ S(\alpha_1,\beta_1,x_m) & ... & S(\alpha_L,\beta_L,x_m) \end{bmatrix}_{m \times L}. \qquad (5)$$

To get the output of $\eta \in R^L$, the rectangular linear system (4) is required to be its minimum norm least square solution. i.e.,

$$\eta = H^{\dagger} y \qquad (6)$$

where $H^{\dagger} H$ is the Moore-Penrose generalized inverse [37] of H.

The output function $f(.)$ is calculated for any new sample $x \in R^n$ as,

$$f(x) = h(x) \cdot \eta$$

(7)

where $h(x) = [(S(\alpha_1,\beta_1,x),...,S(\alpha_L,\beta_L,x))]^t$.

Inspired by the above related work, this study is to create a novel predictive modeling approach using ANN, SVR and ELM to accurately predict BTS. This predictive strength can be harnessed to assist manufacturers in refining their products without the need for conducting extensive large-scale BTS tests in the future.

III. DATASET DESCRIPTION

The dataset used in this research is considered from formerly published work [38]. The dataset consists of 30 samples, with 24 arbitrarily selected as training data and the remaining as testing data. Input variables such as the shorter dimension of bamboo (mm), the longer dimension of bamboo (mm), cross-sectional area (mm^2), Modulus of Elasticity (N/mm^2), and load (kN) which are used to produce the output, i.e., Bamboo Tensile Strength, are presented in Table 1 and Table 2 displays the variable statistics for the "BTS" dataset.

Using the Select Best feature selection method available in the Scikit-learn Python package [39], a feature importance analysis was performed to process the 4 input features. Figure 4 displays the Normalized features of the Bamboo Tensile Strength dataset.

Table 1- Normalized Input Variables for foretelling the "BTS"

Sample No.	Shorter Dimension	Longer Dimension	Area	Load	BTS
1	0.032258	0.583333	0.059668	0	0.234532
2	0.096774	0.583333	0.11002	0.099845	0.317266
3	0.290323	0.458333	0.223313	0.133333	0.197842
4	0.16129	0.375	0.11002	0.133333	0.372662
5	0.16129	0.5	0.140232	0.133333	0.315827
6	0	0.375	0	0.033178	0.458273
7	0.225806	0.416667	0.165408	0.2	0.370504
8	0.387097	0.041667	0.14854	0.6	1
9	0.387097	0.041667	0.14854	0.549767	0.92518
10	0.548387	0	0.21576	0.6	0.802158
11	0.290323	0.416667	0.210725	0.099845	0.170504

12	0.516129	0.25	0.30136	0.133333	0.120144
13	0.290323	0.833333	0.336606	0.366512	0.327338
14	0.580645	0.541667	0.469537	0.366512	0.201439
15	0.387097	0.5	0.307654	0.433178	0.433094
16	1	0.875	1	0.666667	0.109353
17	0.806452	0.5	0.61858	0.549767	0.231655
18	0.83871	1	0.921954	0.733333	0.173381
19	0.774194	0.958333	0.83711	0.899845	0.304317
20	0.677419	0.333333	0.442346	0.283101	0.152518
21	0.548387	0.916667	0.603474	0.533333	0.230216
22	0.677419	0.5	0.52291	0.333333	0.138129
23	0.677419	0.791667	0.663897	0.699845	0.299281
24	0.806452	0.833333	0.799849	0.499845	0.102878
25	0.548387	0.291667	0.339124	1	0.960432
26	0.677419	0.5	0.52291	0.333333	0.138129
27	0.548387	0.916667	0.603474	0.2	0
28	0.806452	0.5	0.61858	0.549767	0.231655
29	0.677419	0.791667	0.663897	0.633178	0.256115
30	0.806452	0.833333	0.799849	0.499845	0.102878

Table 2- Statistics-Summary of the variables in the "Bamboo Tensile strength" dataset

Statistics → Attributes ↓	Shorter Dimension	Longer Dimension	Area	Load	BTS
mean	0.507527	0.548611	0.430178	0.409912	0.32259
std	0.268682	0.278346	0.281031	0.261527	0.262097
25%	0.290323	0.385417	0.176737	0.15	0.157014
50%	0.548387	0.5	0.390735	0.399845	0.233094
75%	0.677419	0.822917	0.61858	0.587442	0.359712
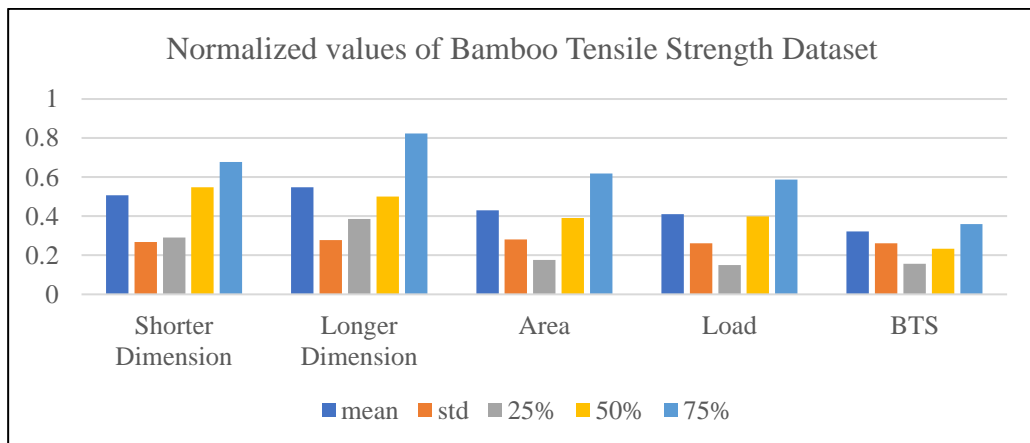
Figure 4: Normalized Features of the Bamboo Tensile Strength Dataset

Table 3 displays correlation coefficients between the variables Shorter Dimension, Longer Dimension, Area, Load, and BTS. It's a symmetric matrix since the correlation between variable X and variable Y is the same as the correlation between variable Y and variable X. The diagonal of the matrix (from the top-left to the bottom-right) contains 1s. This is because a variable's correlation with itself is always 1. In other words, a variable has a perfect positive correlation with itself. On the basis of Table 3 and Figure 5 which display Correlation Matrix Heatmap, let's interpret the matrix as follows:

- *Shorter Dimension and Bamboo Tensile Strength:* The correlation between shorter dimension and BTS is approximately -0.29156. This indicates a weak negative correlation. When the BTS output increases, shorter dimension tends to decrease slightly. However, the correlation is not very strong, and the relationship might not be highly significant.
- *Longer Dimension and Bamboo Tensile Strength:* The correlation between longer dimension and BTS is approximately -0.666212. This indicates a moderate to strong negative correlation. When the BTS output increases, longer dimension tends to decrease significantly. This indicates that there is a more substantial negative connection between longer dimension and bamboo tensile strength.
- *Load and Bamboo Tensile Strength:* The correlation between Load and BTS is 0.351177. This implies a weak positive correlation coefficient. When the bamboo tensile strength output increases, Load tends to increase slightly. Similar to shorter dimension, this correlation coefficient is not very strong, and the connection might not be highly significant.
- *Area and Bamboo Tensile Strength:* The correlation between area and bamboo tensile strength is -0.484018. This implies a moderately negative correlation. When the bamboo tensile strength output increases, the area tends to decrease significantly. This suggests that there is a moderately negative connection between area and bamboo tensile strength.

Table 3: Correlation Coefficient of attributes with the target value

Attributes	Shorter Dimension	Longer Dimension	Area	Load	BTS
Shorter Dimension	1	0.401174	0.917628	0.697998	-0.29156
Longer Dimension	0.401174	1	0.724473	0.207228	-0.666212
Area	0.917628	0.724473	1	0.62101	-0.484018
Load	0.697998	0.207228	0.62101	1	0.351177
BTS	-0.29156	-0.666212	-0.484018	0.351177	1
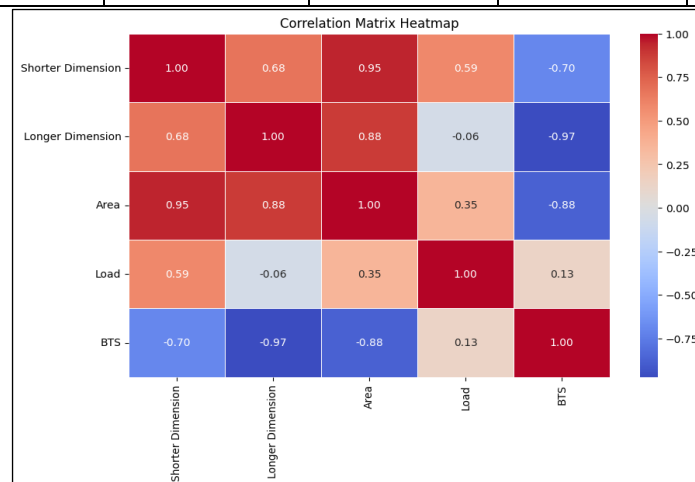
Figure 5: Correlation Matrix Heatmap

IV.   RESULT AND ANALYSIS

In this study, a predictive model is developed using three ML regression algorithms: ELM, SVR, and ANN. The dataset is divided into an 80% training set and a 20% testing set, which is shuffled before use. The optimization process involves minimizing the loss function, with Coefficient of Deformation (R^2) and Mean Square Error (MSE) used as the loss function for this study and the values so obtained are compared with Root Mean Square Error (RMSE) and Mean Absolute Error (MAE).

$$R^2 = 1 - \frac{\sum_{i=1}^{n}(\varepsilon_i - \hat{\varepsilon}_i)^2}{\sum_{i=1}^{n}(\varepsilon_i - \bar{\varepsilon}_i)^2} \tag{8}$$

In the above equation, n is the quantity of specimens. $\varepsilon_i \, and \, \hat{\varepsilon}_i$ are the actual and forecasted values of the target, respectively, of the i_{th} data. $\bar{\varepsilon}_i$ is the mean value of all calculated values.

$$MSE = \frac{1}{n}\sum_{i=1}^{n}(\varepsilon_i - \hat{\varepsilon}_i)^2 \tag{9}$$

$$RMSE = \sqrt{\frac{1}{n}\sum_{i=1}^{n}(\varepsilon_i - \hat{\varepsilon}_i)^2} \tag{10}$$

$$MAE = \frac{1}{n}\sum_{i=1}^{n}\left|\varepsilon_i - \hat{\varepsilon}_i\right| \tag{11}$$

After creating the algorithms, their effectiveness is evaluated by considering various performance metrics, including R^2, MSE, MAE, MAPE, and RMSE as defined in equations (8) to (11). The execution of the developed algorithms on both the training and testing datasets is presented in Table 4. The ELM configuration that demonstrated minimal errors (R^2, MSE, MAE, MAPE, RMSE) and an R^2 value approaching unity was chosen. Out of the 30 input data points, 80% (24 data points) were arbitrarily allocated as the training dataset, while the remaining 20% (6 data points) were used for testing. Figure 6 (a), (b), (c) and Figure 7 showcases a comparison between predicted and actual BTS using various ML techniques, with the coefficient of determination (R^2) serving as the basis for evaluation. Figure 6 (b) & Figure 6 (c) reveal a remarkable resemblance between the SVR and ANN predictions, showcasing a notable non-linearity. This observation is further supported by the performance parameters outlined in Table 4, where the values for both models are nearly identical or near each other. The curve obtained aligned well with the simulated values from the ELM model. Consequently, the "Actual BTS" and "Predicted BTS" graph demonstrates that the ELM algorithm accurately and precisely forecasted the experimentally obtained data.

Table 4: Results based on various performance measures for ELM, SVR, and ANN

Model	Training Dataset	Testing Dataset	Statistical Parameters			
			MSE	R^2	MAE	RMSE
ELM			0.003	0.9966	0.0161	0.018
SVR	24	6	0.0188	0.8007	0.1071	0.137
ANN			0.0313	0.6678	0.1334	0.1768
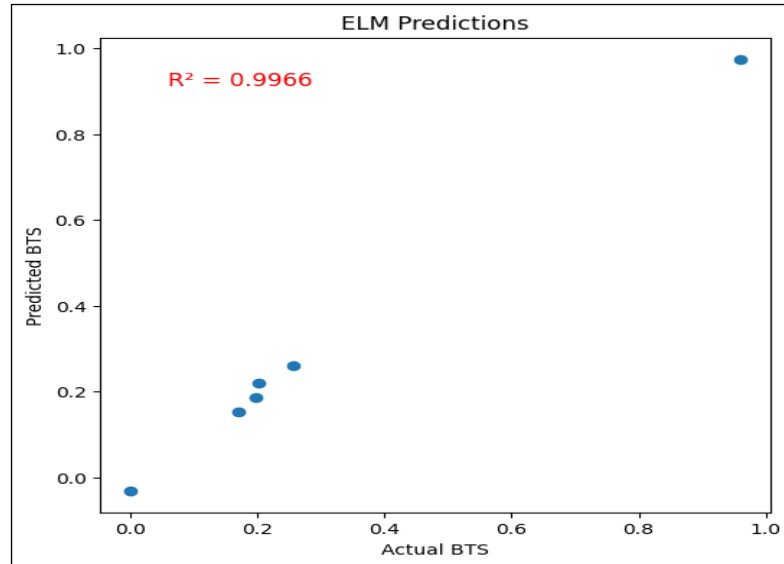
Figure 6 (a)- Extreme Learning Machine Prediction
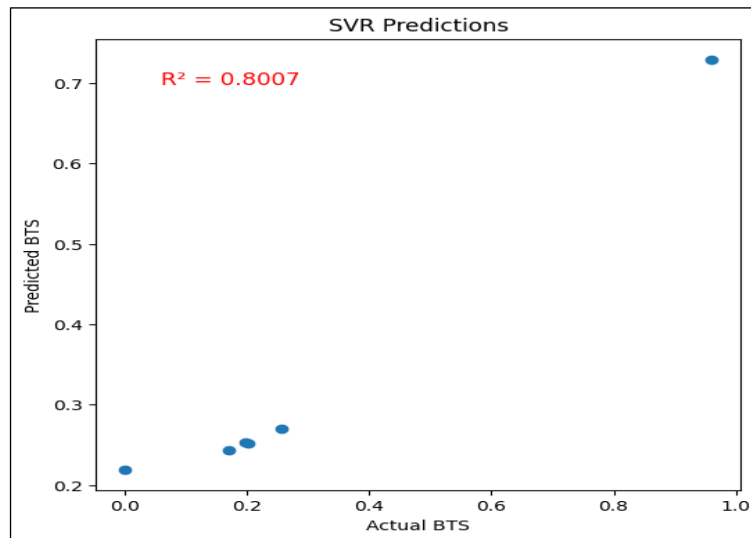
Figure 6 (b)- Support Vector Regression Prediction
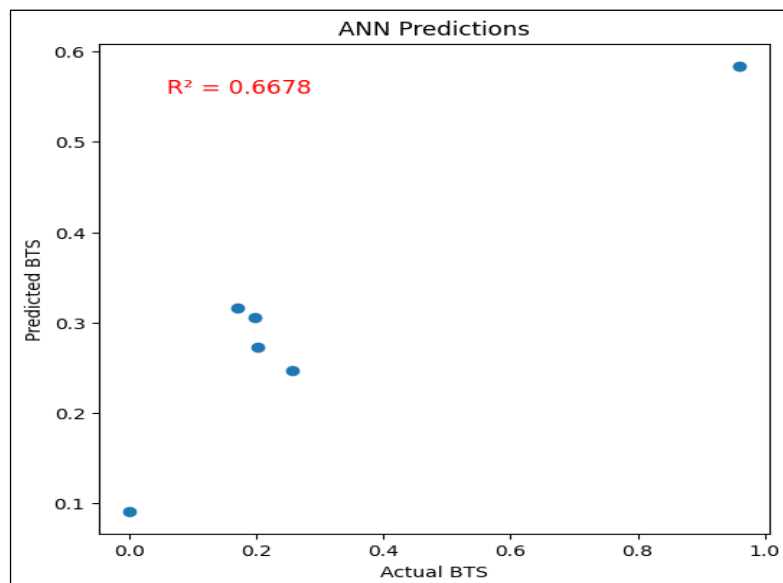
Figure 6 (C)- Artificial Neural Network Prediction
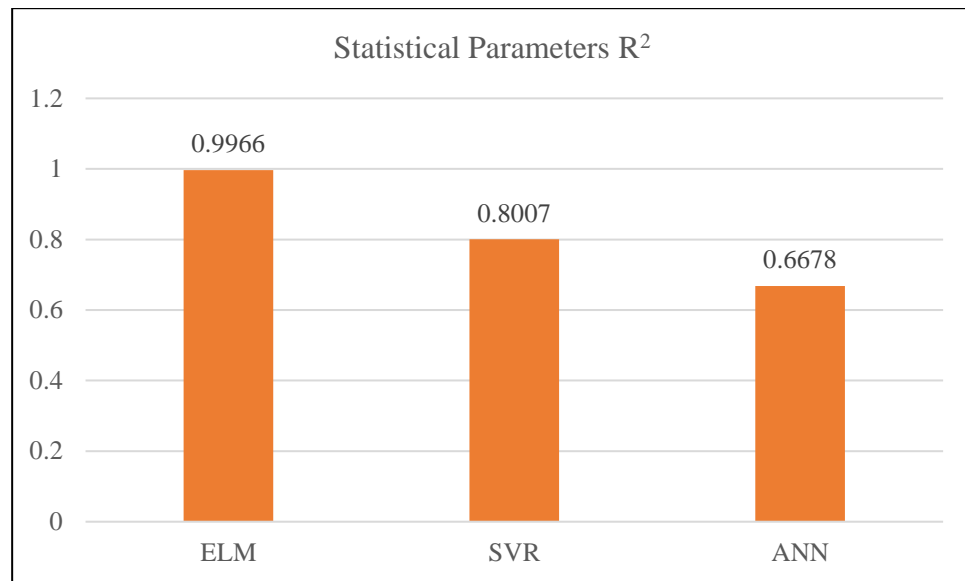
Figure 7- Comparison of Coefficient of deformation of various models on the basis of R^2

V. CONCLUSION AND FUTURE ASPECTS

This research aimed to predict BTS with high precision using the ELM algorithm in combination with ANN and SVR. The research utilized available datasets to validate and calibrate the models, and the outcomes from the ELM algorithm demonstrated a strong correlation with the empirical deflection values observed during experimentation. The mathematical evaluation of the ELM algorithm, incorporating metrics like R^2, RMSE, MSE, MAE, and MAPE, produced highly encouraging outcomes. The R^2 score of 0.9966 signifies an exceptional degree of precision in BTS prediction. Additionally, the RMSE, MSE and MAE values, which stand at 0.018, 0.003 and 0.0161 respectively, reinforce the strength and dependability of the ELM algorithm in its capacity to forecast BTS.

These results imply that the ELM algorithm can serve as a potent tool for foretelling the BTS without necessitating intricate analyses. Furthermore, the knowledge derived from the ELM algorithm and the experimental datasets implies that bamboo holds the potential to substitute traditional steel rebars in civil engineering structures.

To improve the trajectory of this study, future research can consider increasing the dataset size to enhance the accuracy of various ML algorithms. Additionally, researchers could explore the integration of hybrid models, which combine the strengths of different ML algorithms, to further enhance the precision and applicability of BTS estimation. It's worth noting that traditional BTS prediction methods can be computationally expensive and often require a deep understanding of the relationship between features and BTS. However, ML algorithms, such as the ELM algorithm, offer advantages over traditional prediction methods by being able to make accurate predictions without requiring explicit knowledge of the relationship between features and BTS.

REFERENCES

[1]	Bahtiar Effendi Tri 2015 Keandalan Bambu untuk Material Konstruksi Hijau. *Sekolah Pascasarjana Institut Pertanian Bogor*.

[2]	Trujillo David J and L F López 2020 Bamboo material characterisation. *Nonconventional and vernacular construction materials*. Woodhead Publishing: pp. 491-520.

[3]	Fu Yang, Hai Fang, and Fengyu Dai 2017 Study on the properties of the recombinant bamboo by finite element method. *Composites Part B: Engineering* 115: pp.151-159.

[4]	Zhang Han, Haitao Li, Chaokun Hong, Zhenhua Xiong, Rodolfo Lorenzo, Ileana Corbi et.al 2021 Size effect on the compressive strength of laminated bamboo lumber. *Journal of Materials in Civil Engineering* 33(7): 04021161.

[5]	Bahtiar Effendi Tri, Alif Puguh Imanullah, Dede Hermawan, and Naresworo Nugroho 2019 Structural grading of three sympodial bamboo culms subjected to axial compressive load. *Engineering Structures* 181: pp. 233-245.

[6]   Kumar Anuj, Tomáš Vlach, Lenka Laiblova, Martin Hrouda, Bohumil Kasal, Jan Tywoniak, and Petr Hajek 2016 Engineered bamboo scrimber: Influence of density on the mechanical and water absorption properties. *Construction and Building Materials*: pp. 815-827.

[7]   Jakovljević Suzana, Dragutin Lisjak, Željko Alar, and Frano Penava 2017 The influence of humidity on mechanical properties of bamboo for bicycles. *Construction and Building Materials* 150: pp. 35-48.

[8]   Shangguan Weiwei, Yingchun Gong, Rongjun Zhao, and Haiqing Ren 2016 Effects of heat treatment on the properties of bamboo scrimber. *Journal of Wood Science* 62 (5): pp. 383-391.

[9]   Sun Haoxian, Haitao Li, Assima Dauletbek, Rodolfo Lorenzo, Ileana Corbi, Ottavia Corbi, and Mahmud Ashraf 2022 Review on materials and structures inspired by bamboo. *Construction and Building Materials* 325: 126656.

[10]   Liu Wen, Kangning Li and Shilang Xu 2022 Utilizing bamboo biochar in cement mortar as a bio-modifier to improve the compressive strength and crack-resistance fracture ability. *Construction and Building Materials* 327: 126917.

[11]   Zhou Wenjing, Haitao Li, Chen Chen, and Ottavia Corbi 2023 Effect of temperature on axial compressive mechanical properties of bamboo. *Construction and Building Materials* 371: 130734.

[12]   Daud Norhasliya Mohd, Norazman Mohamad Nor, Mohammed Alias Yusof, Azrul Affandhi Mustaffa Al Bakhri, and Amalina Aisyah Shaari 2018 The physical and mechanical properties of treated and untreated Gigantochloa Scortechinii bamboo. In *AIP Conference Proceedings* vol. 1930 (1).

[13]   Li Haitao, Zhenyu Qiu, Gang Wu, Dongdong Wei, Rodolfo Lorenzo, Conggan Yuanet, et.al 2019 Compression behaviors of parallel bamboo strand lumber under static loading. *Journal of Renewable Materials* 7: pp.583-600.

[14]   Baharuddin Norhazaedawati, S Lee, M Anwar Uyup, and P Md Tahir 2022 Effect of preservative treatment on physical and mechanical properties of bamboo (Gigantochloa scortechinii) strips. *BioResources* 17 (3): 5129.

[15]   Althoey Fadi, Paul Oluwaseun Awoyera, King Inyama, Mohammad Arsalan Khan, Mohammad Mursaleen, Haitham M. Hadidi et.al 2022 Strength and microscale properties of bamboo fiber-reinforced concrete modified with natural rubber latex. *Frontiers in Materials* 9: 1064885.

[16]   Gupta Durgesh Kumar and R Singh 2018 An Experimental Evaluation of Compressive Strength and Flexural Strength of Bamboo Fiber Reinforced Concrete. *Carbon* 1.3500: p. 200.

[17]   Yang Dong, Haitao Li, Zhenhua Xiong, Leonel Mimendi, Rodolfo Lorenzo, Ileana Corbi et.al 2020 Mechanical properties of laminated bamboo under off-axis compression. *Composites Part A: Applied Science and Manufacturing* 138: 106042.

[18]   Zhong Yong, Hai Qing Ren, and Ze Hui Jiang 2016 Effects of temperature on the compressive strength parallel to the grain of bamboo scrimbe. *Materials* 9.6: 436.

[19]   Wang Qiuyi, Xinwu Wu, Chenglong Yuan, Zhichao Lou, and Yanjun Li 2020 Effect of saturated steam heat treatment on physical and chemical properties of bamboo. *Molecules* 25(8) :1999.

[20]   Liu Pengcheng, Ping Xiang, Qishi Zhou, Hai Zhang, Jiefu Tian, and Misganu Demis Argaw 2021 Prediction of mechanical properties of structural bamboo and its relationship with growth parameters. *Journal of Renewable Materials* 9 (12): 2223.

[21]   Amelia J J N, Zuhri M Y M, Leman Z, Zahari N I, As Arry A. and Ilyas R A 2021 Quasi-static compression properties of bamboo and pvc tube reinforced polymer foam structures. *Polymers 13*(20): p.3603.

[22]   Huang Yuxiang, Yaohui Ji, and Wenji Yu 2019 Development of bamboo scrimber: A literature review. *Journal of Wood Science* 65 (1): pp. 1-10.

[23]   Hao Xiaomeng, Qiuyi Wang, Yihua Wang, Xin Han, Chenglong Yuan, Yu Cao et.al 2021 The effect of oil heat treatment on biological, mechanical and physical properties of bamboo. *Journal of wood science* 67: pp. 1-14.

[24]   Zhang Xuexia, Jinghao Li, Zixuan Yu, Yan Yu, and Hankun Wang 2017 Compressive failure mechanism and buckling analysis of the graded hierarchical bamboo structure. *Journal of materials science* 52: pp. 6999-7007.

[25]   Zhou Qishi, Jiefu Tian, Pengcheng Liu, and Hai Zhang 2021 Test and prediction of mechanical properties of Moso bamboo. *Journal of Engineered Fibers and Fabrics* 16: 15589250211066802.

[26]   Zagórski I, Kulisz M, Semeniuk A and Malec A 2017 Advances in Science and Technology Research Journal. *Letters* 11(3): pp.261-269.

[27]   McCulloch Warren S and Walter Pitts 1943 A logical calculus of the ideas immanent in nervous activity. *The bulletin of mathematical biophysics* 5: pp. 115-133.

[28]   Firat Mahmut, Mustafa Erkan Turan, and Mehmet Ali Yurdusev 2010 Comparative analysis of neural network techniques for predicting water consumption time series. *Journal of hydrology* 384.1-2: pp. 46-51.

[29]   Abbasi Maryam and Ali El Hanandeh 2016 Forecasting municipal solid waste generation using artificial intelligence modelling approaches. *Waste management* 56: pp.13-22.

[30]   Mashrei Mohammed A, Seracino R, and Rahman M S 2013 Application of artificial neural networks to predict the bond strength of FRP-to-concrete joints. *Construction and Building Materials* 40: pp. 812-821.

[31]   Drucker Harris, Christopher J Burges, Linda Kaufman, Alex Smola, and Vladimir Vapnik 1996 Support vector regression machines. *Advances in neural information processing systems* 9.

[32]   Yuvaraj P, Murthy A R, Iyer N R, Sekar S K. and Samui P 2013 Support vector regression-based models to predict fracture characteristics of high strength and ultra-high strength concrete beams. *Engineering fracture mechanics* 98: pp.29-43.

[33] Hazarika B B, Gupta D, Ashu and Berlin M 2020 A comparative analysis of artificial neural network and support vector regression for river suspended sediment load prediction. In *First International Conference on Sustainable Technologies for Computational Intelligence: Proceedings of ICTSCI*. pp. 339-349.

[34] Cristianini Nello and John Shawe Taylor 2000 *An introduction to support vector machines and other kernel-based learning methods*. Cambridge university press: pp. 93-122.

[35] Huang Guang Bin, Qin Yu Zhu, and Chee Kheong Siew 2006 Extreme learning machine: theory and applications. *Neurocomputing* 70.1-3: pp. 489-501.

[36] Huang Gao, Guang Bin Huang, Shiji Song and Keyou You 2015 Trends in extreme learning machines: A review. *Neural Networks* 61: pp. 32-48.

[37] Rao C R and Mitra S K 1971 Further contributions to the theory of generalized inverse of matrices and its applications. *Sankhyā: The Indian Journal of Statistics, Series A*: pp.289-300.

[38] Mahzuz H M A, Ahmed M, Dutta J and Rose R H 2013 Determination of several properties of a bamboo of Bangladesh. *Journal of Civil Engineering Research 3*(1): pp.16-21.

[39] Pedregosa F, Varoquaux G, Gramfort A, Michel V, Thirion B, Grisel O et.al 2011. Scikit-learn: Machine learning in Python. *the Journal of machine Learning research* 12: pp.2825-2830.